Investigation of Noncontact Optical Image-based Methods for Monitoring of Static and Dynamic Deformation of Transport Infrastructures

Zhijun Wang[1,*], Weijian Li[2], Mingliang Zhao[2]

[1]Key Laboratory of Road Structure & Material, Research Institute of Highway, MOC, Beijing, 100088, China
[2]Shandong Road & Bridge Construction Group Co., Ltd., Jinan, Shandong, 250102, China

*wzjzjy@126.com

Abstract. Deformation properties including displacement is a key factor for determining accurate behavior of transport infrastructures. In this paper, two noncontact methods named 2D and 3D optical measurement methods were developed and tested to measure deformation properties of structures under static and dynamic loading conditions. More advanced cameras including industrial cameras and high-speed cameras were used to improve the efficiency and accuracy of measurement procedure and reduce the processing time. An experimental plan including two experiments considering four different scenarios was designed to provide reliable experimental data, evaluate, and compare the accuracy and efficiency of the proposed optical measurement methods with different configurations. The obtained results approved the reliability and accuracy of all scenarios for deformation measurement of structures. Comparing the results showed that 3D optical image-based method (NRMSE= 4.58) is of more accuracy and capabilities than 2D optical image-based method (NRMSE= 8.47) for both static and dynamic deformation. In addition, the usage of 3D angular camera configuration led to less computational processing and subsequently measurement procedure is accomplished in a more time-saving manner.

Keywords: static and dynamic deformation, measurement, bridge, optical method.

1 Introduction

Nowadays, due to the rapid development and construction of transportation infrastructures, it is necessary to provide higher requirements for their safety [1]. Bridges and slab tracks are the main elements of highway and railway infrastructures that provide the required strength under operational loads. Therefore, knowing the deformation behavior of these elements helps to design and develop safer and more durable structures for operation. Thus far, various kinds of measurement methods including conventional and high-tech methodologies have been proposed for measuring deformation properties of infrastructures.

F. Ding et al. (eds.), *Proceedings of the 2024 International Conference on Civil Engineering Structures and Concrete Materials (CESCM 2024)*, Advances in Engineering Research 247,
https://doi.org/10.2991/978-94-6463-564-5_13

Conventional methods including numerical and contact-based methods have been used for decades to measure structural deformation. In spite of the capability of Numerical methods (i.e. finite element) for estimating deformation properties through making virtual and visual models, they are not more accurate and efficient than the real sensors. In addition, the required computing time for solving problem is high in this case [2]. Dial gauges, wire displacement sensors, and Linear Variable Differential Transformer (LVDT) have been used as accurate contact based methods for deformation measurement of structures [3,4,5,6]. Accelerometer also measures deformation in an indirect way that leads to less accuracy compared with other conventional methods [3,7,8]. Generally, contact-based methods suffer from several deficiencies such as requiring high volume of instruments, and higher cost and time for installation and test implementation as well as much effort and traffic disruption.

High technology devices such as global positioning system (GPS), radar, LiDAR, and vision-based methods have been recently utilized as the noncontact-based method for measurement of deformation properties. GPS provides geolocation and time information to a GPS receiver anywhere on or near the Earth and could measure both long term and instantaneous deformation of structures [9,10,11,12]. Less accuracy and low sampling rate are among the deficiencies of this method. Radar uses radio waves to determine the range (i.e. distance) by measuring the time for the radar signal to propagate to the target and back [13]. LiDAR is a surveying method that can measure distance by illuminating the target with laser light and measuring the reflected light with a sensor. Then the differences in laser return times and wavelengths are used to make 3D coordinates of surrounding scene [14]. However, these devices would take high cost and may not be an optimal solution for full field measurement. In addition, laser exposure is dangerous for people who are dealing with the monitoring procedure.

Among all noncontact-based methods, image-based methods are promising and convenient to address the problem of structural deformation measurement. These methods started to be used at early 90s by measurement of displacement at Humber bridge in UK [15]. Up to now, more evolved methodologies have been examined and investigated to accurately and efficiently measure deformations in both lab and field environment. In spite of previous development in image-based measurement of structural deformation, different challenges still remain requiring deeper investigation. These challenges and their solutions can be considered from different aspects and related to four main parts including camera selection, camera configuration, image data acquisition, and image processing and analysis. Each of these aspects was made progress and evolved during the time of history trying to propose optimal solutions from aspects of accuracy, cost, time, and user friendliness. Cameras from low quality to high quality have been used for both static and dynamic deformation measurement of infrastructures. Generally, there are two main factors that may differentiate cameras in terms of accuracy for deformation measurement: camera resolution and frame rate. Usually, camera resolution and frame rate are selected depending on the experimental conditions such as structural vibration frequency, distance from camera to structure, and deformation type (static or dynamic). Higher camera resolution and frame rate leads to higher accuracy. However, there may be exceptions in some cases [16]. There is a relationship between camera resolution and frame rate. The highest resolution can be achieved using

nominal camera frame rate. As the camera frame rate increases higher than nominal frame rate, the image resolution will be decreased and subsequently leads to less accuracy. So far, various kinds of cameras including webcams, digital cameras, and industrial cameras have been adapted to gather image data for deformation measurement. In case of requiring higher frame rate, the camera frame rate was increased higher than nominal frame rate to detect and estimate deformation of higher frequency structural vibration. Based on the definition of high-speed camera, it is capable of capturing moving images with exposures of less than 1/1,000 second. Deformation measurement of transport infrastructures has not been performed by high-speed camera using its nominal frame rate with its maximum achievable resolution. One of the aims of this study is to examine image-based methods by high-speed cameras using nominal frame rate for measurement of bridge dynamic deformation and compare their performance with other utilized cameras. Previous studies tested various camera configurations for deformation measurement including single camera, dual camera, and multiple camera systems. Each of these configurations may have different capabilities and advantages compared with others. The other aim of this study is to design and implement single and dual camera configurations and evaluate their performance and capabilities in measurement of structural deformation from aspects of time, cost and accuracy. Image data acquisition is also accomplished through different manners including manual or automatic ways. Since it is required to make a stationary platform during image data acquisition for achieving accurate results, automatic image data capturing is superior compared with manual methods. This challenge was also considered and explained in this study. Since leveraging suitable image processing and analysis algorithms is vital for achieving accurate deformation results, various algorithms have been tested and developed to calculate in-plane and out-of-plane deformation of structures depending on the type of camera configuration system and captured image specifications. Based on the above mentioned facts, we are aiming to investigate, address, and discuss the above mentioned challenges and their solutions through development and implementation of reproducible 2D and 3D optical image-based methods.

This work is dedicated to the development and execution of a non-contact optical sensing algorithm to measure infrastructure structure deformation considering the camera motion. The method handles ambient camera vibrations without any additional optical equipment, or the time and cost of setting up additional independent reference systems/points, or arranging additional monitoring programs. Then, the proposed methods are verified and validated by designing an experimental plan including two different experiments on concrete beam and bridge model. Finally, the obtained results are presented and the effects of various factors such as camera type, camera configuration, image data acquisition methods, and the performance of image processing and analysis algorithms are discussed.

2 Strategy of Deformation Measurement

Image-based system is able to measure and track the physical position of any target point in the surrounding scene through processing and analyzing successive images

which are captured by cameras. This system consists of two main components including Image data acquisition platform and image processing and analysis toolbox. The first component includes cameras and their accessories, targets, checkerboard, computer, and image acquisition software while the second component is composed of various kinds of algorithms and approaches that are used to extract the necessary information from images for camera calibration and target detection and tracking by analysis of image sequence. So, each of these parts are well designed to establish an accurate deformation measurement system that is described in the following.

2.1 Image Data Acquisition Platform

The image data acquisition system utilizes two types of cameras including industrial cameras (UI 3370 CP; resolution: 2048×2048; frame rate: 75 fps) and high-speed cameras (Fastcam SA3 Model 120K; resolution: 1024×1024; frame rate: 2000 fps). High-speed cameras are able to capture images with higher frame rate at reduced image resolution (e.g. up to 120,000 fps). Circular black targets are installed on the structure to be detected and tracked for measurement of static and dynamic deformation. A square checkerboard (12×9 @ 26 mm) is used for camera calibration. In this study, two kinds of camera configuration are investigated: mono camera configuration and dual camera configuration. In the former, single camera is used to obtain the image data while in the later two cameras are placed in an angular orientation relative to each other so that all the measurement area on the structure surface can be detectable by both cameras. Given the type of camera configuration, there are different image analysis approaches for tracking target points that are described in the following section.

2.2 Image-based Tracking System

Target tracking is usually performed either within 2D plane or in 3D space. In mono camera configuration, successive monitoring images are taken using single camera so that the first image is considered as the reference image, the target point is tracked within the 2D image plane, and subsequently deformation is calculated by analysis of image sequence. In dual camera configuration, two similar cameras are placed in parallel or angular orientation, and capture monitoring images at the same time with the same resolution and frame rate. Likewise, the first couple of images are considered as the reference images. Then, 3D position of target points are estimated during the time of loading and subsequently structural deformation (static or dynamic) is calculated. In this study, it is assumed that all the installed cameras are stationary and are not subjected to any kinds of movement. Totally, two sets of images are captured during data gathering: calibration images which are taken before the main experiment and monitoring images which are taken during the experiment when the static or dynamic loads are applied. Each of these sets of images are separately processed and analyzed to estimate the camera calibration parameters and subsequently calculate the target movements and structural deformation. Based on the above mentioned facts, two different procedures called 2D and 3D optical image-based methods are proposed in this study to analyze image data and measure deformation of structures using mono and dual

angular camera configuration systems. Fig. 1 describes the architecture of the proposed measurement methodology.

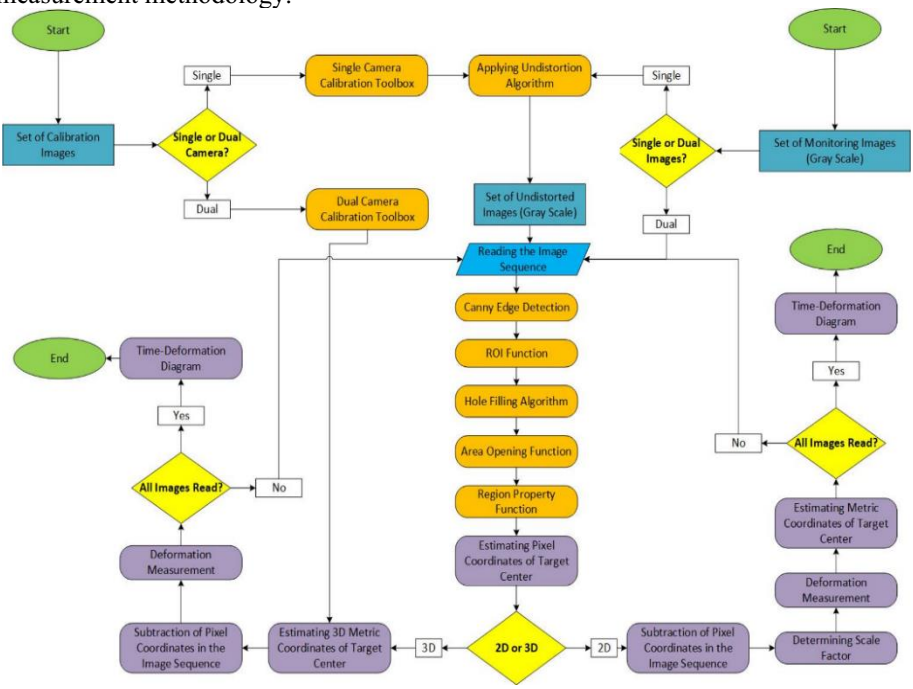

Fig. 1. Architecture of the proposed optical image-based methods

2.3 2D Optical Image-based Method

2D optical image-based method is developed to measure 2D structural deformation under static and dynamic loading conditions using a single camera. The analysis procedure starts with estimation of camera calibration parameters by minimizing the following functional [17]:

$$\min_{K,R^n,t^n} \sum_{j,n} \left\| \hat{x}_j^n - p(K[R^n \;\; t^n]\tilde{X}_j^o) \right\|^2 \tag{1}$$

where $\hat{x}_j^n$ is the image of node j location in the dewarped image plane. K is the camera calibration matrix, R^n is the rotation matrix, t^n characterize the position of the checkerboard in the project domain, and $\tilde{X}_j^o$ is the coordinate of physical point in the local coordinate system.

Having estimated camera calibration parameters, the algorithm of image distortion correction is applied to remove the lens distortion and produce gray scale undistorted images [18]. The first image is considered as the reference image and then is analyzed to detect and determine the target center position using a robust image processing and analysis algorithm as follows: Stage 1: The operator of Canny edge detection is applied to detect edges in an image while suppressing noise [19]. Stage 2: Region of interest

(ROI) function is used to create a portion of an image for filtering or performing other operations. Stage 3: Hole filling algorithm is adapted to fill a confined region using a special color or pattern [20]. Stage 4: Area opening function removes all thin protrusions from objects and open up a gap between objects connected by a thin bridge without shrinking the objects [21]. Stage 5: Finally, region property function is used to measure a set of properties of each connected object including the centroid point [21].

Accordingly, the pixel coordinates of target centers are calculated. Likewise, all the successive images are processed and analyzed one by one and the coordinates of target canters at each image are subtracted from the ones in preceding image. The image scale factor is a constant value which is calculated to convert the pixel deformation value to metric value based on the following equation:

$$SF = \frac{P_n}{I_n} \tag{2}$$

Where, P_n is the metric diameter of circular target and I_n is the target diameter in pixel. Having estimated pixel deformation and image scale factor, metric coordinates of target centers are calculated by following the same procedure for all images. Accordingly, all the successive images are analyzed for estimation of momentary metric position of target centers. Having the pixel position of each target center on the image at time {t, t+1, t+2, t+3, … , t+n} that correspond to $\{(x_t, y_t), (x_{t+2}, y_{t+2}), (x_{t+2}, y_{t+2}), (x_{t+3}, y_{t+3}), \dots, (x_{t+n}, y_{t+n})\}$and the image scale factor SF, the metric position of each target center is calculated through the following equation:

$$\begin{bmatrix} X_{t+n} \\ Y_{t+n} \end{bmatrix} = \begin{bmatrix} X_t \\ Y_t \end{bmatrix} + SF \begin{bmatrix} x_{t+n} - x_t \\ y_{t+n} - y_t \end{bmatrix} \tag{3}$$

Where (X_t, Y_t) and (X_{t+n}, Y_{t+n}) are the metric position of each target center at time t and $(t + n)$.

2.4 3D Optical Image-based Method

This method is developed to measure static and dynamic in-plane and out-of-plane deformation of the structures using two cameras as shown in Fig. 1. In this study, the cameras are angularly adjusted. Both calibration and monitoring images are captured through an automated image acquisition application. The 3D camera calibration procedure is applied in order to determine the camera intrinsic and extrinsic parameters using MATLAB calibration app.

In order to estimate the 2D position of each target center within the successive pairs of images (captured by left and right cameras), the proposed 5-phase image processing and analysis method described in section 2.3 is applied. Based on the proposed image processing and analysis algorithm, the targets are detected and tracked within the image plane of both left (x_l, y_l) and right images (x_r, y_r). Accordingly, all image pairs $\{i = 1,2,3, \dots, n\}$ are processes and analyzed and 2D position of all targets are calculated. The next stage is to calculate the 3D position of each target center in real world coordinate system (X_n, Y_n, Z_n) using the following equations:

$$X_n = \frac{x_l . Z_n}{f_l} \tag{4}$$

$$Y_n = \frac{y_l . Z_n}{f_l} \tag{5}$$

$$Z_n = \frac{f_l(f_r t_x - x_r t_z)}{x_r(r_7 x_l + r_8 y_l + f_l r_9) - f_r(r_1 x_l + r_2 y_l + f_l r_3)} = \frac{f_l(f_r t_y - y_r t_z)}{y_r(r_7 x_l + r_8 y_l + f_l r_9) - f_r(r_4 x_l + r_5 y_l + f_l r_6)} \tag{6}$$

where f_l and f_r are the focal length of the left and right camera, (x_l, y_l) is the pixel location of target center in the left image, (x_r, y_r) is the pixel location of target center in the right image. With estimating 3D coordinate of each target center over the time, the momentary 3D metric position of target center can be calculated by the following equation:

$$\begin{bmatrix} X_{t+k} \\ Y_{t+k} \\ Z_{t+k} \end{bmatrix} = \begin{bmatrix} X_t \\ Y_t \\ Z_t \end{bmatrix} + \begin{bmatrix} X_{t+k} - X_t \\ Y_{t+k} - Y_t \\ Z_{t+k} - Z_t \end{bmatrix} \tag{7}$$

where (X_t, Y_t, Z_t) and $(X_{t+k}, Y_{t+k}, Z_{t+k})$ is 3D metric position of each target center at time t and $t + k$.

3 Experimental Study

Two experimental study including concrete beam test and bridge model experiment were conducted to investigate the accuracy and performance of the proposed 2D and 3D optical image-based methods. These experiments were described in the following sections.

3.1 Concrete Beam Experiment

In this experiment, the reliability of the proposed 2D and 3D optical image-based methods were verified through the concrete beam test. This test was conducted to measure the deformation of the concrete beam under static loading condition. A concrete beam (dimension: $0.8 \times 0.3 \times 0.2\ m$) was loaded continuously by the MTS testing machine. The experimental setup including the optical camera configuration and concrete beam setup is shown in Fig. 2. This beam is a part of a slab track made in the lab based on the characteristics of concrete railway slab track that is currently used in Beijing-Shanghai high-speed railway in China [22]. The size of the whole slab in the lab is $6.45m \times 2.55m \times 0.2m$. Then, we cut the slab in transverse and longitudinal directions and made the above-described concrete beam (Fig. 2a~c).

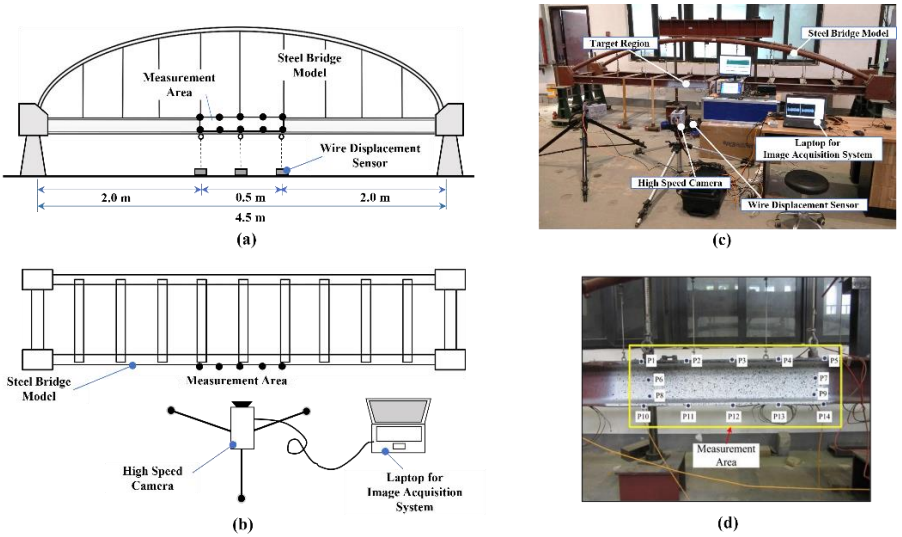

Fig. 2. Description of verification experiment for optical sensing measurement system: The steel bridge model and targets set (front view) (a), Arrangement of optical sensing measurement system (overhead view) (b), Experimental site (full view) (c), and (b) Concrete beam set up

The continuous static vertical load was applied at the top center of the beam while the monitoring images were captured simultaneously by the mounted optical system. The gauge connected to MTS testing machine actuator also recorded the true value of deformation at the top center of the beam. The optical instruments including industrial cameras (Model: UI 3370 CP, Maximum frame rate: 75 fps, Sensor size: 2048*2048 pixels, and Pixel size: 5.5 μm), black circular target (Diameter: 15 mm), checkerboard (Dimension: 12×9 @$26\ mm$), and laptop (Intel core i5-5200U @ 2.20 GHz, RAM: 8GB) have been utilized to collect the image data through a data acquisition software. Targets of K_1, K_2, K_3, and K_4 were installed in four different points on the side surface of the concrete beam in order to be detected and tracked for measurement of concrete beam deformation. The utilized industrial camera and the general view of data acquisition application is shown in Fig. 3.

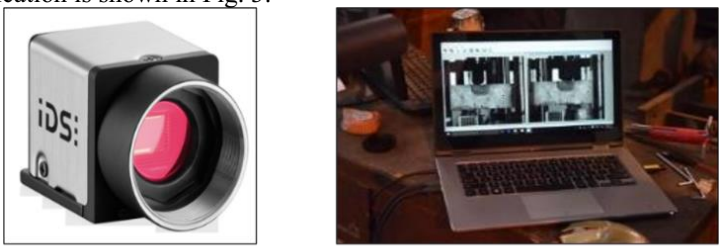

Fig. 3. Image data acquisition equipment: (a) Industrial Camera (Model: UI 3370 CP) and (b) Image data acquisition application

The static load is continuously applied until the concrete beam is broken. The industrial cameras simultaneously captured the measurement images for about several minutes. All the obtained images were stored directly on the hard drive of the laptop. Finally, both 2D and 3D optical image-based methods were applied to measure in-plane vertical deformation of the concrete beam under static load conditions.

3.2 Bridge Model Experiment

A bridge model experiment was conducted to verify the accuracy and efficiency of the proposed 2D and 3D optical image-based methods and compare their reliability for measurement of bridge deformation under dynamic loading conditions in the lab. This model is a 4.5 m-long single-span steel arch bridge that consists of eleven small girders with the distance of 0.45 m. A measurement area of 0.45 m was selected in the central part of the bridge model to be investigated for deformation measurement. Fourteen black circular targets (diameter: 15 mm) were installed on the surface of this area to be detected and tracked. Two high-speed cameras (Fastcam SA3 Model 120K, frame rate: 1000 fps, resolution: 1024×1024) were utilized to collect the image data. The high-speed cameras were angularly adjusted. A square checkerboard (Dimension: 12×9 @$26\ mm$) was also used for camera calibration. The experimental setup including optical camera system and the measurement area are shown in Fig. 2. As indicated in Fig. 2b, the measurement area was highlighted by the white color. The distance between two successive targets along the horizontal direction is almost equal to 11.25 cm. The relative position of the cameras is angular almost at 45 degrees with the horizontal direction. The cameras were located almost 1.5 m away from bridge model. Suitable illumination were also provided using two sources of light.

The impact hammer was used to manually apply the dynamic load on the center point of the bridge model which is associated with the dynamic response of the bridge that last for a few seconds. Wire displacement sensors were also used to measure the true values of the bridge vertical dynamic deformation. A data logger was connected to wire displacement sensors. Three wire displacement sensors installed at three locations of targets $P_{10}, P_{12},$ and P_{14} to measure the real vertical dynamic deformation of bridge model. The utilized high-speed cameras and the wire displacement sensors are shown in Fig. 4.

To start the experiment, calibration images were taken. Then the bridge model was induced by the impact hammer and dynamic load was applied three times. The high-speed cameras simultaneously captured the measurement images for about 8 seconds. The obtained images were transformed and stored on the hard drive of the laptop. Finally, image data were processed and analyzed and the vertical deformation of bridge model was estimated using both 2D and 3D optical image-based methods and compared. Totally, 8188 images were captured and among all, 500 images were analyzed to estimate dynamic deformation during the first second of bridge dynamic response.

Fig. 4. Data acquisition equipment: (a) High-speed camera (b) Wire displacement sensor

4 Results and Discussion

4.1 Concrete Beam Experiment

The results of image data analysis are presented in this section. MATLAB camera calibration app was used to perform the camera calibration procedure.

The results of both 2D and 3D camera calibration are shown in Table 1.

Table 1. Camera calibration results (Camera Model: UI 3370 CP)

2D calibration results		**3D calibration results**	
Camera focal length	9119.5	Left camera focal length	9472.3
		Right camera focal length	9348
Skew	$\gamma = 0$	Skew	$\gamma = 0$
Camera principle point	$u_0 = 953.2204$ $v_0 = 956.1578$	Left camera principle point	$u_0 = 947.03$ $v_0 = 916.23$
		Right camera principle point	$u_0 = 963.90$ $v_0 = 983.39$
Camera lens distortion (radial)	$k_1 = 0.3362$ $k_2 = -7.6536$	Left camera lens distortion (radial)	$k_1 = 0.314$ $k_2 = 3.859$
		Right camera lens distortion (radial)	$k_1 = 3.859$ $k_2 = 6.235$
		Relative camera rotation	$\begin{matrix} 0.9866 & 0.0028 & -0.1626 \\ -0.0012 & 0.9999 & 0.0098 \\ 0.1626 & -0.0094 & 0.9866 \end{matrix}$
		Relative camera translation (mm)	$[-397.22\ 0.033\ 1.88\ ]$

Followed by the estimation of camera calibration parameters and removing image distortion, circular targets were detected and their center positions were determined by

processing and analyzing image sequence. Fig. 5 illustrates the procedure of image processing and analysis applied on a sample captured image of concrete beam.

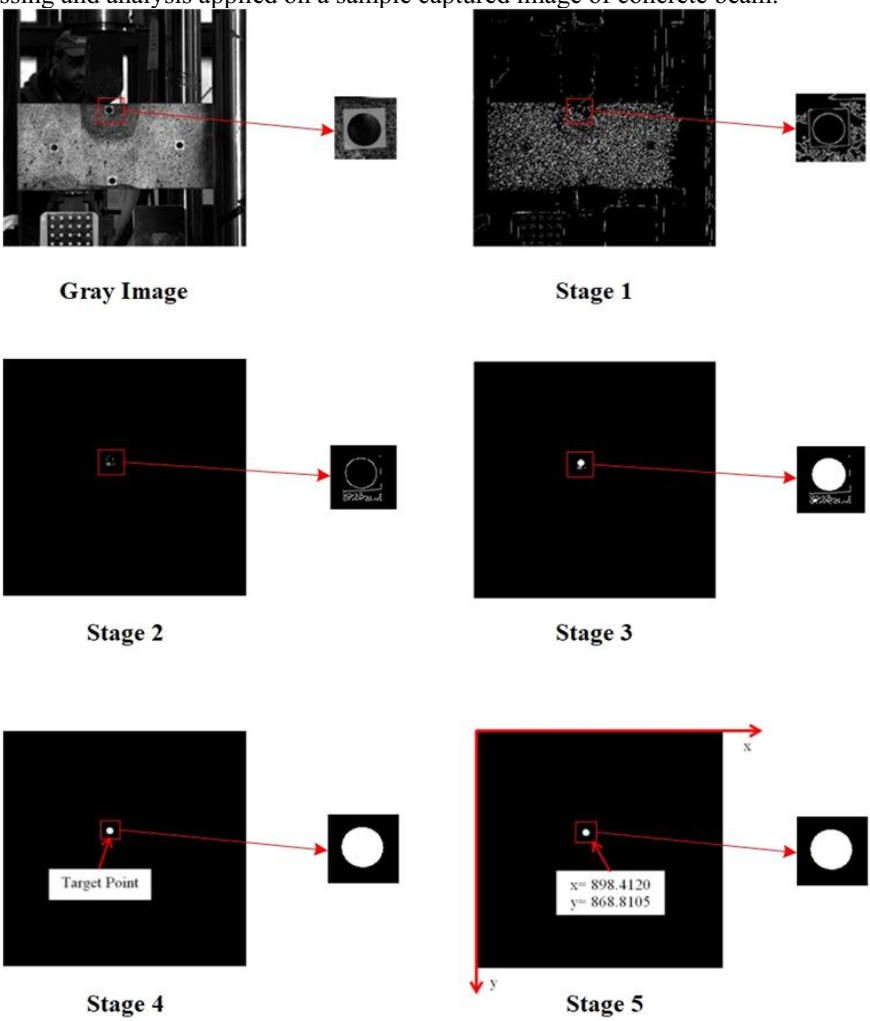

Fig. 5. Illustrate the performance of image processing and analysis algorithm

Finally, 2D and 3D momentary metric position of each target center in real world coordinate system was calculated and the time-deformation relationship was obtained. The results of concrete beam vertical deformation at targets K_1, K_2, K_3, and K_4 obtained through 2D and 3D optical image-based methods are shown in Fig. 6. Comparing the results of 2D and 3D optical measurement methods with those obtained through MTS machine actuator proved the accuracy of the proposed methods for static deformation measurement. Two measures of goodness including Root Mean Square Error (RMSE), and Normal Root Mean Square Error (NRMSE) have been used to quantify the deviation between measured and estimated deformation.

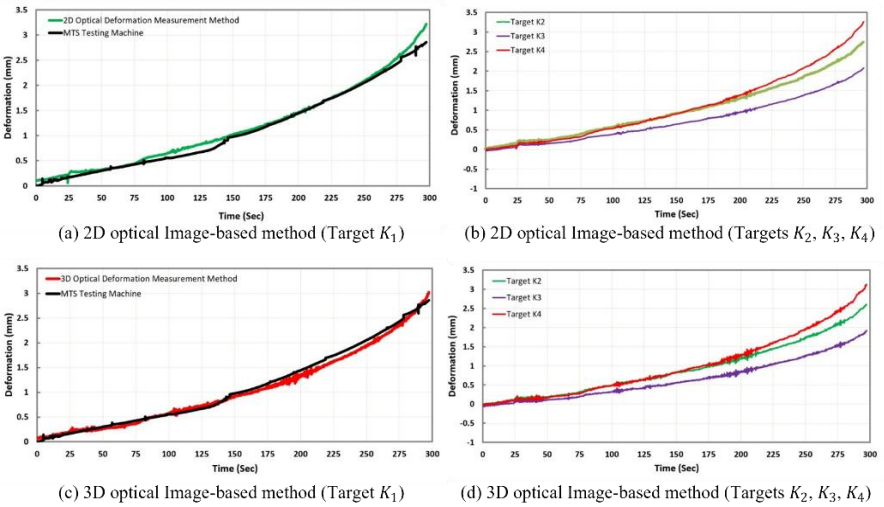

(a) 2D optical Image-based method (Target K_1) (b) 2D optical Image-based method (Targets K_2, K_3, K_4)

(c) 3D optical Image-based method (Target K_1) (d) 3D optical Image-based method (Targets K_2, K_3, K_4)

Fig. 6. Time- vertical deformation at targets K_1 to K_4 using 2D and 3D optical image-based methods

The results of measurement error are shown in Table 2. As can be found from this Table, 3D optical image-based method was found more accurate than 2D optical image-based method.

Table 2. Measurement error at targets K_1

Method	2D optical image-based	3D optical image-based
Deformation Type	Vertical	Vertical
RMSE (mm)	0.192	0.094
NRMSE (%)	7.40	3.63

4.2 Bridge Model Experiment

The analysis stage started by estimation of camera calibration parameters as shown in Table 3. Based on the procedure of 2D and 3D optical image-based methods, all the collected images obtained from bridge model were processed and analyzed. Dynamic vertical deformation was estimated at targets P_{10}, P_{12}, and P_{14} where the wire displacement sensors measured the real deformations. Then, the achieved deformation results from analysis of images were compared with those obtained through wire displacement sensors.

The diagrams of time-deformation using angular camera configuration at targets P_{10}, P_{12}, and P_{14} were illustrated in Fig. 7. In this Figure, the obtained results of dynamic bridge deformation by 2D and 3D optical image-based methods were compared with those obtained by wire displacement sensors. With this comparison, it was found that the deformation results of 2D and 3D optical image-based methods agree with

ground-truth values obtained by wire displacement sensor. The calculated measurement errors (RMSE and NRMSE) indicated the accuracy and efficiency of the proposed methods as shown in Table 4. Based on the deformation results in Table 4, it was concluded that 3D optical image-based method is more accurate (max error= 4.58%) than 2D optical image-based method (max error=8.47%) for measurement of bridge dynamic deformation in this study.

Table 3. Camera calibration parameters (Camera Model: Fastcam SA3 Model 120K)

2D calibration results		**3D calibration results**	
Camera focal length	3093.72	Left camera focal length	9472.3
		Right camera focal length	9348
Skew	$\gamma = 0.745$	Skew	$\gamma = 0$
Camera principle point	$u_0 = 489.77$ $v_0 = 601.55$	Left camera principle point	$u_0 = 484$ $v_0 = 602.47$
		Right camera principle point	$u_0 = 505.64$ $v_0 = 607.31$
Camera lens distortion (radial)	$k_1 = 0.3362$ $k_2 = -7.6536$	Left camera lens distortion (radial)	$k_1 = -0.109$ $k_2 = -1.758$
		Right camera lens distortion (radial)	$k_1 = -0.149$ $k_2 = 1.560$
		Relative camera rotation	$\begin{bmatrix} 0.7997 & -0.0137 & -0.6003 \\ 0.0177 & 0.9998 & 0.0007 \\ 0.6002 & -0.0113 & 0.7998 \end{bmatrix}$
		Relative camera translation (mm)	$[-1064.33 \quad 12.12 \quad 316.46]$

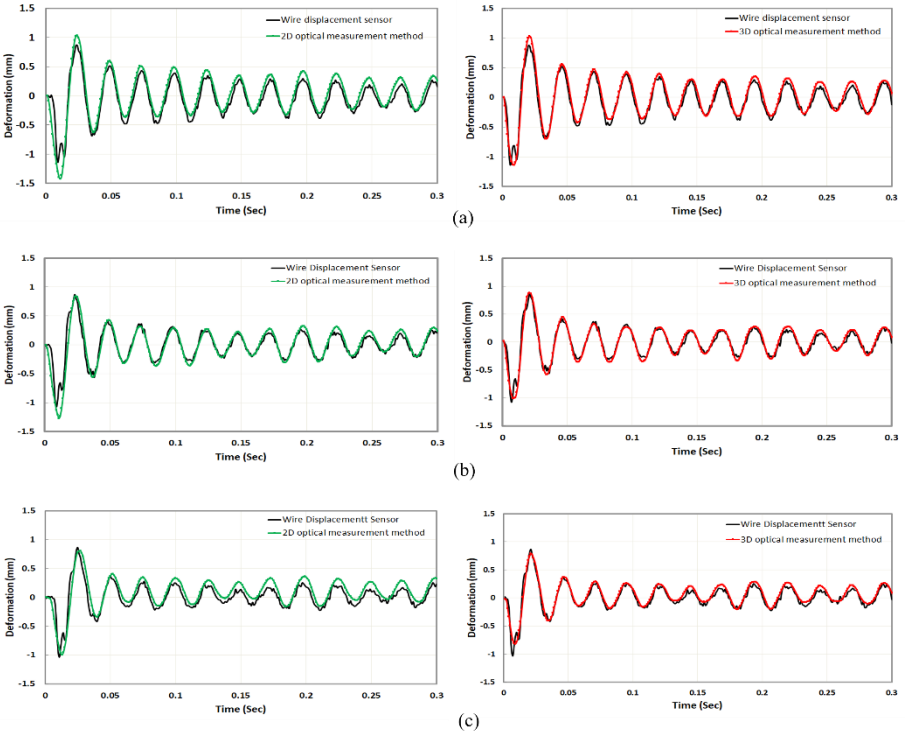

Fig. 7. Diagrams of time-vertical deformation using 2D and 3D optical image-based methods: (a) at target P_{10}; (b) at target P_{12}; (c) at target P_{14}

Generally, four different scenarios has been investigated in this study based on the proposed experimental plan, which is described in Table 5.

As can be seen, all the measurement scenarios led to accurate estimation of deformation that indicates the accuracy and efficiency of both 2D and 3D optical image-based methods for measurement of both static and dynamic deformation. Therefore, it is concluded the proposed optical image-based methods can be considered as a suitable replacement for conventional measurement methods.

Table 4. Deformation measurement error

2D Optical image-based method			
Target ID	Camera Configuration	RMSE (mm)	NRMSE (%)
Target P_{10}	Single Camera	0.170	8.47
Target P_{12}		0.128	6.55
Target P_{14}		0.140	7.38
3D Optical image-based method			
Target P_{10}	Dual Camera (angular)	0.092	4.58
Target P_{12}		0.070	3.59
Target P_{14}		0.061	3.20

Table 5. Scenarios of deformation measurement

Load type	Structure	Utilized Camera	Deformation Type	Optical Camera Configuration	Measurement Method	Scenario ID	NRMSE (%)
Static	Concrete Beam	Industrial Camera	Vertical	Dual Camera (angular)	3D Optical	Scenario 1	3.63
				Single Camera	2D Optical	Scenario 2	7.40
Dynamic	Bridge Model	High-Speed Cameras	Vertical	Dual Cameras (angular)	3D Optical	Scenario 3	4.58
				Single Camera	2D Optical	Scenario 4	8.47

According to the obtained results, 3D optical image-based method achieved the highest accuracy for estimation of static deformation of concrete beam. Although 3D optical image-based method is of higher accuracy, however, it might need more equipment, more time and cost to be installed. Therefore, this configuration should be selected according to the requirements of the experiment. This method is usually utilized when out-of-plane deformation is going to be measured.

Two different types of cameras have been used in this study including industrial cameras Model: UI 3370 CP), and high-speed cameras (FASTCAM SA3 Model 120) [23,24]. Both camera types have shown successful performance. However, higher accuracy was achieved using industrial cameras that might be because of its higher image resolution. It is noted that cameras with higher frame rate are used to measure deformation of structure with higher vibration frequency.

In addition, two different optical configuration including single camera and dual camera systems have been set up for image data acquisition. As indicated in Table 5, the obtained accuracy from dual camera system is higher than single camera system that showed more reliable performance of the former system. However, single camera system is less expensive, more time-effective, and less capable.

From aspect of image data acquisition, maximum frame rate for both industrial (75 fps) and high-speed cameras (1000 fps) was adjusted to collect image data. Reaching the highest image frame rate also depends on the specifications of the data acquisition devices such as laptop or other related accessories such as data loggers and cables that may cause to provide less frame rate. It should be mentioned that higher frame rate than nominal camera frame rate could be provided if the image resolution decreases.

5 Conclusions

In this study, two methods of 2D and 3D optical image-based methods were developed to measure static and dynamic deformation of structures. Two experiments including concrete beam and bridge model tests were conducted to evaluate the proposed methods under static and dynamic loading conditions. The obtained results showed the accuracy

and successful performance of both proposed methods. Based on the experimental design, four scenarios were investigated and compared. The comparison results indicated 3D optical image-based method is of higher accuracy specially for static deformation measurement. The highest accuracy was achieved for 3D optical image-based method in order to measure static deformation (NRMSE= 3.63). More issues have also been considered in this study including utilizing different camera types (Industrial and high-speed cameras), camera configuration systems (Single and dual camera systems), and data acquisition system. Based on the above mentioned issues, several findings were achieved:

(1) More accurate results were obtained using industrial cameras in this study. Industrial cameras were able to take images with higher resolution than high-speed cameras and this leads to achieving more accurate deformation results. In addition, they are less expensive and the installation time of industrial cameras are quite less than high-speed cameras. Moreover, data acquisition procedure is done more conveniently by industrial cameras than high-speed cameras.

(2) Single camera configuration was more accurate according to the results of this study. It is also preferable when the installation time and cost is important for implementation of optical deformation measurement method. However, dual camera configuration is of more capabilities than single camera configuration such as measurement of out-of-plane deformation.

(3) Robust image processing and analysis algorithm was another advantage of the proposed methods. This algorithm could compensate the poor performance of cameras or low resolution of images to achieve the high accuracy results.

(4) Dynamic deformation could be measured successfully through high-speed cameras in the presence of high frequency dynamic loading conditions. Although high-speed cameras are useful in this case, however, it is much more expensive than the other camera types.

This study provides a potential solution to the problem of the monitoring device's own vibration affecting the test results in computer-visual structural monitoring. However, the current validation tests were conducted in the laboratory only, and the further research will apply the system for structural deformation monitoring in the field and compare it with conventional methods.

References

1. Lee, J.; Kim, R.E. Noncontact dynamic displacements measurements for structural identification using a multi-channel Lidar. Struct. Control Heal. Monit. 2022, e3100.
2. Entezami, A.; Arslan, A.N.; De Michele, C.; Behkamal, B. Online Hybrid Learning Methods for Real-Time Structural Health Monitoring Using Remote Sensing and Small Displacement Data. Remote Sens. 2022, 14.
3. Klarák, J.; Andok, R.; Hricko, J.; Klačková, I.; Tsai, H.Y. Design of the Automated Calibration Process for an Experimental Laser Inspection Stand. Sensors 2022, 22.
4. Ghyabi, M.; Timber, L.C.; Jahangiri, G.; Lattanzi, D.; Shenton III, H.W.; Chajes, M.J.; Head, M.H. Vision-Based Measurements to Quantify Bridge Deformations. J. Bridg. Eng. 2023, 28, 5022010.

5. Kassem E, Grasley Z, Masad E. Viscoelastic Poisson's ratio of asphalt mixtures. Int J Geomech 2013; 13(2): 162–9.
6. Li, Y.H. and Liu, J.P. A new convergence monitoring system for tunnel or drift based on draw-wire displacement sensors. Tunnelling and Underground Space Technology, 2015, 49, pp.92-97.
7. Park JW, Sim SH, Jung HJ. Development of a wireless displacement measurement system using acceleration responses. Sensors. 2013 Jul;13(7):8377-92.
8. H. Wang, T. Tao, T. Guo, J. Li, A. Li, Full-scale measurements and system identification on sutong cable-stayed bridge during typhoon Fung-Wong, Sci. World J. 2014, 13
9. Meng, X.; Roberts, G.W.; Cosser, E.; Dodson, A.H.; Barnes, J.; Rizos, C. Real-time bridge deflection and vibration monitoring using an integrated GPS/Accelerometer/Pseudolite System. In Proceedings of the 11th International Symposium on Deformation Measurements, Santorini, Greece, 25–28 May 2003; Volume 6, pp. 25–28.
10. Meng, X.; Dodson, A.H.; Roberts, G.W. Detecting bridge dynamics with GPS and triaxial accelerometers. Eng. Struct. 2007, 29, 3178–3184.
11. Moschas, F.; Stiros, S. Measurement of the dynamic displacements and of the modal frequencies of a short-span pedestrian bridge using GPS and an accelerometer. Eng. Struct. 2011, 33, 10–17.
12. Handayani, H.H.; Taufik, M. Preliminary study of bridge deformation monitoring using GPS and CRP (case study: Suramadu Bridge). Procedia Environ. Sci. 2015, 24, 266–276.
13. Gentile, C. and Bernardini, G. An interferometric radar for non-contact measurement of deflections on civil engineering structures: laboratory and full-scale tests. Structure and Infrastructure Engineering, 2010. 6(5), pp.521-534.
14. Liu W, Chen SE, Boyajian D, Hauser E. Application of 3D LiDAR scan of a bridge under static load testing. Materials evaluation. 2010 Dec 1;68(12):1359-67
15. Stephen GA, Brownjohn JM, Taylor CA. Measurements of static and dynamic displacement from visual monitoring of the Humber Bridge. Engineering Structures. 1993 Jan 1;15(3):197-208
16. L. Sun, V. Abolhasannejad, L. Gao, Y. Li, Non-contact optical sensing of asphalt mixture deformation using 3D stereo vision, Measurement, 2016, 85, 100– 117.
17. Muller K, Hemelrijk CK, Westerweel J, Tam DS. Calibration of multiple cameras for large-scale experiments using a freely moving calibration target. Experiments in Fluids. 2020 Jan 1;61(1):7.
18. Solof SM, Adrian RJ, Liu ZC. Distortion compensation for generalized stereoscopic particle image velocimetry. Meas Sci Technol, 1997, 8(12):1441–1454
19. Xuan L, Hong Z. An improved canny edge detection algorithm. In2017 8th IEEE international conference on software engineering and service science (ICSESS) 2017 Nov 24 (pp. 275-278). IEEE.
20. Zhao H, Chen ZX. A Simple Hole Filling Algorithm for Binary Cell Images. InApplied Mechanics and Materials 2013 (Vol. 433, pp. 1715-1719). Trans Tech Publications Ltd.
21. Marques O. Practical image and video processing using MATLAB. John Wiley & Sons; 2011 Aug 4.
22. Gomez, F.; Narazaki, Y.; Hoskere, V.; Spencer, B.F.; Smith, M.D. Bayesian inference of dense structural response using vision-based measurements. *Eng. Struct.* 2022, *256*, 113970.
23. Wu, Z.; Chen, G.; Ding, Q.; Yuan, B.; Yang, X. Three-dimensional reconstruction-based vibration measurement of bridge model using uavs. *Appl. Sci.* 2021, *11*.
24. Chen, G.; Liang, Q.; Zhong, W.; Gao, X.; Cui, F. Homography-based measurement of bridge vibration using UAV and DIC method. *Meas. J. Int. Meas. Confed.* 2021, *170*, 108683.